

This is the accepted version of the following article:

Langevin D., Lozano O., Salvati A., Kestens V., Monopoli M., Raspaud E., Mariot S., Salonen A., Thomas S., Driessens M., Haase A., Nelissen I., Smisdom N., Pompa P.P., Maiorano G., Puntes V., Puchowicz D., Stepnik M., Suárez G., Riediker M., Benetti F., Mi. Inter-laboratory comparison of nanoparticle size measurements using dynamic light scattering and differential centrifugal sedimentation. *NanoImpact*, (2018). 10. : 97 - . 10.1016/j.impact.2017.12.004,

which has been published in final form at  
<https://dx.doi.org/10.1016/j.impact.2017.12.004> ©  
<https://dx.doi.org/10.1016/j.impact.2017.12.004>. This  
manuscript version is made available under the CC-BY-NC-ND  
4.0 license  
<http://creativecommons.org/licenses/by-nc-nd/4.0/>

# Inter-laboratory comparison of nanoparticle size measurements using dynamic light scattering and differential centrifugal sedimentation.

D. Langevin<sup>1</sup>, O. Lozano<sup>2,3</sup>, A. Salvati<sup>4,5</sup>, V. Kestens<sup>6</sup>, M. Monopoli<sup>4,7</sup>,  
 E. Raspaud<sup>1</sup>, S. Mariot<sup>1</sup>, A. Salonen<sup>1</sup>, S. Thomas<sup>4</sup>, M. Driessens<sup>8</sup>, A. Haase<sup>8</sup>, I. Nelissen<sup>9</sup>, N. Smisdom<sup>9</sup>  
 P.P. Pompa<sup>10</sup>, G. Maiorano<sup>10</sup>, V. Puntes<sup>11</sup>  
 D. Puchowicz<sup>12</sup>, M. Stępnik<sup>13</sup>, G. Suárez<sup>14</sup>, M. Riediker<sup>14,15</sup>, F. Benetti<sup>16</sup>, I. Mičetić<sup>16</sup>, M. Venturini<sup>16</sup>,  
 W.G. Kreyling<sup>17</sup>, M. van der Zande<sup>18</sup>, H. Bouwmeester<sup>18</sup>, S. Milani<sup>19</sup>, J. Raedler<sup>19</sup>, S.  
 Mülhopt<sup>20</sup>, I. Lynch<sup>21</sup>, K. Dawson<sup>4</sup>

1. Laboratoire de Physique des Solides, CNRS UMR 8502, Université Paris Sud 11, Université Paris Saclay, Orsay, France
2. Namur Nanosafety Centre (NNC), Namur Research Institute for Life Sciences (NARILIS), Research Centre for the Physics of Matter and Radiation (PMR), University of Namur, Namur, Belgium.
3. Cátedra de Cardiología y Medicina Vascular, Escuela de Medicina y Ciencias de la Salud. Tecnológico de Monterrey. Monterrey, México.
4. Centre for BioNano Interactions, University College Dublin, Dublin 4, Ireland
5. Groningen Research Institute of Pharmacy, University of Groningen, Groningen, the Netherlands
6. European Commission, Joint Research Centre (JRC), Geel, Belgium
7. RCSI Pharmaceutical and Medical Chemistry, Royal College of Surgeons in Ireland, Dublin 2, Ireland
8. German Federal Institute for Risk Assessment, Department of Chemical and Product Safety, Berlin, Germany
9. Flemish Institute for Technological Research (VITO), Unit Environmental Risk and Health, Mol, Belgium.
10. Istituto Italiano di Tecnologia (IIT), Via Morego 30, Genoa, Italy
11. Inorganic NPs Group, Institut Català de Nanociència i Nanotecnologia, Bellaterra (Barcelona) Spain and Institut Català Recerca i Estudis Avançats (ICREA), Barcelona, Spain
12. Scientific Department of Unconventional Technologies and Textiles, Textile Research Institute, Łódź, Poland
13. Dept of Toxicology and Carcinogenesis, Nofer Institute of Occupational Medicine, Łódź, Poland
14. Institut universitaire romand de Santé au Travail, Epalinges-Lausanne, Switzerland
- 15a. SAFENANO, IOM (Institute of Occupational Medicine), Singapore Pte Ltd, Singapore
- 15b. School of Materials Science & Engineering, Nanyang Technological University, Singapore
16. ECSIN-European Center for the Sustainable Impact of Nanotechnology, ECAMRICERT SRL, Rovigo, Italy

17. Helmholtz Centre Munich – German Research Center for Environmental Health, Institute of Epidemiology 2, Neuherberg / Munich, Germany
18. RIKILT – Wageningen University & Research Centre, Wageningen, the Netherlands.
19. Soft condensed matter physics, CeNS & Faculty of Physics, Ludwig-Maximilians-University, München, Germany
20. Karlsruhe Institute of Technology (KIT); Institute for Technical Chemistry (ITC) Eggenstein-Leopoldshafen, Germany
21. School of Geography, Earth and Environmental Sciences, University of Birmingham, Edgbaston, United Kingdom

## Abstract

Nanoparticle in vitro toxicity studies often report contradictory results with one main reason being insufficient material characterization. In particular the characterization in biological media remains challenging. Our aim was to provide robust protocols for two of the most commonly applied techniques for particle sizing, i.e. dynamic light scattering (DLS) and differential centrifugal sedimentation (DCS) that should be readily applicable also for users not specialized in nanoparticle physico-chemical characterization. A large number of participants (about 40) were recruited for a series of inter-laboratory comparison (ILC) studies covering many different instrument types, commercial and custom-built, as another possible source of variation. ILCs were organized in a consecutive manner starting with dispersions in water employing well-characterized spherical silica (19 and 100 nm diameter) and two types of functionalized spherical polystyrene particles (50 nm diameter). At first each laboratory used their in-house established procedures demonstrating high overall variability particularly for the small silica particles (measured diameters between 10 and 50nm), emphasizing the need for standard operating procedures (SOPs). SOPs have been developed by four expert laboratories but were tested for robustness by a large number of users in a second ILC (11 for DLS and 4 for DCS). In a similar approach another SOP for complex biological fluids, i.e. cell culture medium containing serum was developed, again confirmed via an ILC with 8 DLS and participating laboratories.

Our study confirms that reliable data depend on well-established SOPs which have to be optimized for each dispersant. SOPs may be developed by a small number of expert laboratories but for their widespread applicability they need to be verified by a larger number of laboratories.

## 1. Introduction

Nanotechnologies are developing rapidly in areas such as information technology, biotechnologies, advanced materials with tailored properties, and energy storage. In these applications, nano-objects play a central role. For instance, nanotubes are incorporated into materials to improve their conductivity or mechanical resistance, silica and titania nanoparticles (NPs) are popular additives in food and cosmetics, quantum dots are important in the development of next-generation displays, and perovskite, as well as titania NPs, are increasingly used in energy storage devices. The use of NPs in medical applications is also dramatically increasing, as new “smart” particles are capable of site-specific drug targeting and releasing the drugs in a controlled fashion<sup>1</sup>. Despite their immense potentials, several studies have addressed the potential hazard of NPs for human health and the environment. While the majority of NPs are considered non-toxic, a growing concern of possible adverse health effects has stimulated considerable research worldwide, providing new insights about their interaction with biological species<sup>2</sup>.

Evidently, various parameters affect the impact of NPs on living systems. Not necessarily the particle size, but rather the total surface area, which for a given concentration is larger for smaller particles, can be a determinant of NP impact<sup>3</sup>. Numerous contributions have been published in the last 20 years on this topic, often yielding contradictory results. In several European Union Research and Innovation Framework Programmes (FP7) and Horizon 2020, as well as in NanoSafety Cluster projects, the precise role of NP size remains a strong focus. The potential toxicity of NPs has to be evaluated on a case by case basis, with the size not being the only parameter, the shape of the particles also appearing important. For example, small carbon nanotubes are considered more toxic than spherical particles, particularly in pulmonary studies<sup>4</sup>. Of course, toxicity is not exclusively dictated by the particle size and shape, but it also depends on the particle material and coating, its porosity, crystallinity, heterogeneity, roughness and even strain of bonds between surface groups, as well as on the dissolution rate and dispersion state<sup>5</sup>.

However, the determination of particle size is highly important in toxicity studies. Not only to characterize the starting material, but also to provide information on the colloidal stability of the dispersions as applied to cell-based *in-vitro* assays, where buffers of high ionic strength are typically used and are supplemented with proteins, as a source of nutrients for the cells. This information is relevant from both scientific and regulatory viewpoints. Moreover, exposure to such complex media drastically changes NP properties such as size and surface charge, due to the adsorption of biomolecules from the media on the NP surface, resulting in a very different outcome and impact on cells<sup>6</sup>. Exposure to biological fluids can also lead to particle instability and agglomeration. It is foreseen that well-dispersed NPs and agglomerates can exhibit a significantly different cellular response<sup>7</sup>. Recent studies demonstrate that particle- and media-dependent agglomeration in cell culture media can impact the time required for NPs to be internalized by cells in culture, with subsequent effects on hazard rankings<sup>8</sup>. Thus, accurate and reproducible size measurements also constitute a critical step to better understand and estimate particle transport *in vitro*, and the particle dose delivered to cells over time.

Various techniques, based on different underlying physical measurement principles are available for particle size analysis. The most commonly used are electron and scanning probe microscopy (for dry samples), X-ray scattering, resistive pulse sensing, light scattering and centrifugation aided

sedimentation<sup>9</sup>. Dynamic light scattering (DLS) was developed in the 1960's and many bench top instruments are now commercially available and widely used. Differential centrifugal sedimentation (DCS), also referred to as line-start incremental centrifugal liquid sedimentation, is another useful technique that provides high-resolution information on monodisperse and polydisperse samples, when also dispersed in complex media<sup>10</sup>. Each of these methods presents some advantages and limitations against each other, and not all of the methods are suited to characterize NP dispersions in biological fluids. DLS is well established and easy to use for homogeneously dispersed samples. The presence of few large particles such as aggregates or agglomerates can, however, dominate the intensity of the scattered light signal, obscuring the presence of the smaller constituent particles. Even very few agglomerates can be detected because the intensity of scattered light increases with the diameter to the power of six. As a result, experienced users are required to interpret the results and extrapolate meaningful information on the NP size. Despite this limitation, DLS proved to be a reliable technique, providing valuable information on the size distribution of NP dispersions, even in biological fluids when no agglomeration occurs<sup>11</sup>. DCS, on the contrary, is a less common technique; however, emerging studies reveal that it is capable of resolving the presence of multiple populations of particles (according to their sedimentation rate), for instance in strongly agglomerated samples when the NPs are exposed to biological or environmental media<sup>9a,10</sup>. Even in the presence of agglomerates, the non-agglomerated NPs can still be detected. The DCS method is however not suited to measure the size of agglomerates accurately, unless the effective density of the agglomerates can be reliably determined. Due to their different physical measurement principles, both DLS and DCS techniques are therefore highly complementary<sup>12</sup>. It should be mentioned that the accuracy and comparability of DLS and DCS results directly depend on the accuracy of the values of the different input quantities occurring in the corresponding measurement models (as it will be discussed in Sections 2.2 and 2.3, the parameters that must be known in DLS are the scattering angle, temperature and viscosity and in DCS, the density and size of calibration particles, the density of the test particles, and the density of the liquid).

DLS and DCS are considered as suitable methods and commonly used for routine particle size analysis. Both techniques were used within the QualityNano project, a European Union 7<sup>th</sup> Framework Programme research infrastructure (Grant INFRA-2010-262163) for developing best practices and innovation in nanomaterial health and safety testing. One central activity of QualityNano has been the establishment of quality assurance and quality control conditions for nanomaterial safety and assessment. One of the first steps undertaken was to investigate inter-laboratory, inter-batch, and multi-user variations when measuring the size of NPs in simple buffers or in complex biological media such as those typically used for cell culture. This paper describes a series of inter-laboratory comparison (ILC) studies of NP size measurements performed by means of DLS and DCS.

Since 2010, different ILC studies have been organized in the field of NP characterization. Some of the first of their kind were the ILC studies organized by Lamberty et al. and Roebben et al<sup>13</sup>. During the ILC study by Lamberty et al., a reference material which consisted of a near-monodisperse population of near-spherical silica NPs of nominally 35 nm in diameter, and dispersed in an aqueous solution, was analyzed by 38 laboratories using different particle size and zeta potential measurement methods. In contrast to most classical ILC studies, laboratories had to analyze the reference material provided according to their in-house established measurement procedures, i.e. without common measurement instructions. The results obtained were used by the ILC organizer to

evaluate the performance of the laboratories with respect to their measurement and reporting expertise. The laboratories that scored satisfactorily were qualified to participate in later ILC studies aiming at the characterization of candidate certified reference materials<sup>14</sup>. The ILC study set up by Roebben et al. aimed at studying the potential biological impact of nanomaterials by measuring the NP size and zeta potential of selected test materials such as gold, silica, ceria and polystyrene NPs. The results revealed that if laboratories used a sufficiently detailed protocol, reproducible results could be obtained for near-monodisperse systems. Measurements on polydisperse systems containing agglomerates appeared to be problematic, even when following a specific and agreed procedure. Another study, which is more similar to the approach discussed in this contribution, and also within the framework of the QualityNano research infrastructure, was organized by Hole et al. in 2013<sup>15</sup>. In that study, the reproducibility of a particle tracking analysis (PTA) method was studied. The ILC study consisted of different rounds; no guidelines were provided to the participants during the first round, while detailed protocols had to be followed in the subsequent rounds. The results showed that by following a common measurement protocol the inter-laboratory variability improved from about 40 % during round 1 to about 5 % during round 4.

The present work extends this approach to other NPs, other dispersants (including cell culture medium containing serum) and larger variety of instruments provided by several participating laboratories. In contrast, during the ILC study organized by Hole et al., all the participants used instruments from the same manufacturer.

As a first step and related to the findings in the study by Hole et al., we show that even for apparently straightforward measurements of NPs dispersed in a simple matrix such as water, significant variability can be obtained in independent laboratories when common protocols or instructions for the dispersion preparation and measurement are missing. To correct such variability, we then used a series of ILC studies to develop and optimize robust standard operating procedures (SOPs) for NP measurements in water and in a representative cell culture media containing serum, used for *in vitro* NP cell testing, based on the examples provided in previous work<sup>15</sup>. The SOPs were developed and optimized through preliminary tests between three laboratories with the aim of identifying and highlighting crucial steps that could lead to potential discrepancies between the laboratory results. Also, all method parameter values that are crucial for obtaining accurate and comparable results were fixed in the SOPs. The ILC results obtained using the developed SOPs showed a remarkable agreement for both techniques, as well as for DLS measurements in cell culture media, thus that ILCs are a powerful tool to test inter-laboratory variability and that SOPs can be developed and optimized to achieve high quality in nanosafety testing.

## 2. Materials and methods

### 2.1 Nanoparticles

NPs, which are known to be easily dispersed in water and cell culture medium containing serum, were specifically selected to test variability in NP sizing across independent laboratories. Dispersions of monodisperse silica NPs were obtained from the European Commission's Joint Research Centre (JRC, Geel, Belgium). These NPs (ERM-FD100) have a certified diameter of  $(19.0 \pm 0.6)$  nm and  $(20.1 \pm 1.3)$  nm (measured with the DLS cumulants and DCS methods, respectively) and are dispersed in an aqueous solution containing a small amount of NaOH as a stabilizing agent (pH = 9). The nominal particle mass fraction in the suspension of ERM-FD100 is 10 mg/mL. It must be noted that in the frame of the conducted ILC studies the original material was diluted in purified water to a nominal concentration of 1 mg/mL. The diluted material was then split into different sub-samples which were then transferred to other sample containers. Under such conditions, the certified values are no longer guaranteed. Hence, in this paper, the material is further referred to as 19 nm silica instead of ERM-FD100. Additional NPs were acquired from Polysciences, Inc. This material consists of silica NPs of nominally 100 nm in diameter suspended in an aqueous solution (catalog number 24041). According to the manufacturer, these NPs have a nominal diameter of 100 nm.

Monodisperse aqueous dispersions of polystyrene (PS) NPs with amine (PS-NH<sub>2</sub>) and carboxyl (PS-COOH) surface functionalization and nominal 50 nm in diameter were bought from Bangs Laboratories (catalog number PA02N) and Polysciences, Inc. (catalog number 15913-10), respectively. PS-NH<sub>2</sub> was included as a potential positive control for NP-induced cytotoxicity (due to its positive surface charge, it is expected to exhibit biological impacts)<sup>16</sup>. The suspending medium contains a small amount of residual surfactant from the synthesis, which acts as a stabilizing agent.

For all the NPs tested, samples were derived from a single one before the start of each ILC round. This was to ensure that all participating laboratories received aliquots of the same materials, prepared in the same way from the same stocks and all pre-diluted in purified water (resistivity of 18.2 MΩ.cm at 25 °C) to a final concentration of 1 mg/mL. The DLS ILC rounds 1 and 2, and the DCS ILC rounds, were carried out using the same particle samples dispersed in purified water.

For DLS Round 3, NPs were dispersed in cell culture medium containing serum, as used when testing NP behavior and its impact on standard cell lines *in vitro*. More specifically in this case, modified eagle medium (MEM) enriched with glutamax (Invitrogen, Cat. # 41090093) was used and supplemented with 10 % Fetal Bovine Serum (FBS, Gibco catalog number 10270), non-heat inactivated and 100 U/mL Penicillin / 100 µg/mL streptomycin (Invitrogen Cat. #15070063). The full details on media preparation can be found in the SOP which is included in the Supplementary Information. For this round in cell culture medium containing serum, all NPs were measured to a final concentration of 100 µg/mL, as described in the SOP (see Supplementary Information).

### 2.2 DLS background

DLS instruments measure the intensity autocorrelation function  $g_2(\tau)$  of the scattered light intensity,  $I$ , at time  $t$ <sup>17</sup>:  $g_2(\tau) = \langle I(t) I(t + \tau) \rangle$ . When the particles are spherical and monodisperse:

$$g_2(t) = 1 + \exp(-t/\tau) \quad (1)$$

with

$$\tau = 1/(2Dq^2) \quad (2)$$

$D$  being the translational diffusion coefficient and  $q$  the wave vector:  $q = 4\pi n \sin(\theta/2)/\lambda$ , where  $n$  is the solution refractive index,  $\theta$  the scattering angle and  $\lambda$  the wavelength (in vacuum) of the incident laser light. If the dispersions are dilute so that interactions between particles can be neglected,  $D$  is given by the Stokes-Einstein formula:

$$D = \frac{k_B T}{6\pi\eta R_h} \quad (3)$$

$k_B$  is the Boltzmann constant,  $T$  the absolute temperature,  $\eta$  the dynamic viscosity of the dispersing medium and  $R_h$  the hydrodynamic radius. In general, a little error is made in calculating the particle radius with the Stokes formula when the particles are not strongly charged and when their volume fraction is less than or close to about 1 %<sup>18</sup>.

In practice, particle populations are never perfectly monodisperse. As a result, the correlation function is a superposition of functions corresponding to the different particle sizes. When the polydispersity is not too high, the correlation function can be written as a *cumulant* expansion:

$$\ln[g_2(\tau) - 1] \approx -\frac{t}{\tau} + \frac{\mu_2}{2} \left(\frac{t}{\tau}\right)^2 \quad (4)$$

where  $\mu_2/2$  is the polydispersity index (PDI). For a Gaussian distribution around a mean radius  $\bar{R}$ :

$$f(R) = \frac{1}{\sigma\sqrt{2\pi}} e^{-\frac{(R-\bar{R})^2}{2\sigma^2}} \quad (5)$$

the PDI is equal to  $\sigma$ .

### 2.3. DCS background

The DCS technique measures the sedimentation time of particles. Sample dispersions are injected into the center of a spinning disc. Under typical operation, the disc is loaded with a sucrose density gradient solution of known viscosity and density. Under these conditions, the dispersed particles will separate according to differences in size and density (also according to their shape when the particles are not spherical). The time  $t$  elapsed from the injection of the sample until the particles are detected by the turbidity detector is measured. The equivalent hydrodynamic radii of the particles are calculated using Stokes' law:

$$R_h = \sqrt{\frac{9\eta \ln\left(\frac{r_f}{r_0}\right)}{2t(\rho_p - \rho_f)\omega^2}} \quad (6)$$

where  $\eta$  is the dynamic viscosity of the dispersing medium,  $r_f$  is the radial position of the detector,  $r_0$  is the radial position of the front of the density gradient,  $\rho_p$  is the effective particle density,  $\rho_f$  is the fluid density and  $\omega$  is the angular frequency. It should also be noted here that the effective average density of formed agglomerates can be significantly lower than that of the non-agglomerated constituent particles. The methods to characterize the density of agglomerates dispersed in physiological media and used for *in vitro* toxicity studies have been proposed recently<sup>19</sup>.

Throughout a measurement series, the physical properties of the density gradient change due to the constantly increasing volume of fluid in the disc. To ensure the reliability of the DCS results, the properties of the gradient, as well as the ratio  $r_f$  to  $r_0$ , must be accurately re-assessed prior to each new measurement. This is a challenging task, also because the currently available DCS instruments cannot control the temperature inside the disc. It is well-known that due to frictional heating, this temperature can be about 7 °C above ambient temperature. To overcome these measurement challenges, an alternative approach based on calibrating the measurement sedimentation time scale with spherical particles of known size and effective density is commonly applied<sup>20</sup>.

## 2.4 Participants equipment

Eighteen laboratories participated in the first DLS ILC. Five different commercial instruments were used by laboratories 1-13, laboratory 14, laboratory 15 and laboratory 16, respectively. Laboratories 17 and 18 used customized DLS setups. More details can be found in the SI (Table S4). Three commercial instruments performed size measurements in back-scattering conditions (fixed scattering angle 173°). The other commercial instrument (16) and the customized instruments (17 and 18) instead allowed varying the scattering angle. Participants 16 and 17 used a scattering angle of 90°, while participant 18 worked at various angles (30°, 40°, 70°, 90° and 120°) in testing the validity of equation 2. The subsequent ILC rounds, DLS measurements were performed using only commercial instruments and working in back-scattering conditions.

For DCS, a total of three ILC rounds were held, in which three, four and six laboratories participated, respectively. All the laboratories used DC24000 or DC20000 instruments from CPS Instruments, Inc.

## 2.5 Measurements and statistical analysis

For DLS measurements, the average hydrodynamic diameter and PDI were obtained from the correlation functions using a cumulant analysis (scattered light intensity-weighted harmonic mean hydrodynamic diameter, also referred to as z-average diameter). The instrument software programs also calculate size distributions using mathematical inversion procedures such as CONTIN and NNLS. The results obtained from these algorithms are generally characterized by larger measurement uncertainties because the reliability of the inversion procedures is significantly affected by the signal-to-noise ratio<sup>21</sup>. For DCS measurements, the hydrodynamic diameter was obtained from the mass-weighted modal diameter.

The variability arising from the preparation of the NP test samples was estimated by preparing from each sample, three separate and independent aliquots from each sample. Three replicate measurements (by DLS and/or DCS) were then performed on each aliquot, corresponding to a total of nine reported measurement results per sample.

The DLS and DCS results were analyzed based on their arithmetic mean and standard deviation (SD) using a weighted scheme. The weighted mean is defined as :

$$x = \frac{\sum_{i=1}^n w_i x_i}{\sum_{i=1}^n w_i} \quad (7)$$

Here, the weight  $w_i$  was taken as  $1/(SD_i)^2$  for each laboratory measurement. Thus, laboratories with high dispersion values have a lower weight and contribute less to the weighted mean. This scheme

provides more robust values than regular mean and standard deviation calculations by placing less importance on highly scattered data.

According to the documentary standard ISO/IEC 17043:2010, a laboratory's result (mean value  $\pm$  SD) is acceptable if it falls within the assigned range (ILC consensus value  $\pm 2 \times$  SD). In our ILC studies, the consensus value for a given ILC dataset corresponds to the global average calculated from the results of the participating laboratories. In each figure, the global average is accompanied with a pair of dashed lines which define the interval in which the results are expected to fall assuming a confidence level of 95 %. The coefficient of variation (CV) is defined as the ratio between the standard deviation and the global average.

### 3. Results and discussion

#### 3.1 DLS results

##### 3.1.1 DLS of NP dispersions in water.

Interlaboratory comparisons (ILCs) are a powerful instrument to identify any limitations and issues in reproducibility of measurements in independent laboratories. Within the QualityNano Research Infrastructure, we have used ILCs to investigate reproducibility in NP size measurements. As a first step, we selected a panel of well-characterized NPs of different sizes and compositions. To this aim, commercially available 19 nm and 100 nm silica, and 50 nm carboxylated and amino-modified polystyrene NPs were selected. The same stocks were used to prepare simple dispersions in water that were shipped to all participating laboratories. DLS is a rather common technique available in most NP testing laboratories. In fact, 18 different laboratories participated in this test; hence representing a rather high number and it also allowed comparison of results obtained on the samples with different instruments (as detailed in the Materials and methods section and the Supplementary Information). Participating laboratories were asked to perform measurements on the 19 nm silica, 50 nm PS-NH<sub>2</sub> and PS-COOH NP samples by using their in-house developed measurement procedure, i.e. without using a common SOP. The results obtained were rather surprising and highlighted that even for simple measurements in water, and especially for the smaller NPs that are more prone to agglomeration, the results were highly variable. The results for the 19 nm silica, 50 nm PS-NH<sub>2</sub> and 50 nm PS-COOH NP samples are shown in Figure 1, 2a and 2b respectively. The NP size measurements were conducted using the cumulants method.

After the analysis, the data spread for the 19 nm silica NP sample was considerable, with reported size values ranging from 7 nm to 45 nm (data not shown). During the data scrutinization, it became clear that some laboratories had reported radii instead of diameter values for the particle size. While this data inconsistency could be easily resolved, it already shows that a common understanding of certain measurement terms, such as 'particle size', which can have a variety of meanings, is vital when comparing measurement results. Converting the identified radii result into their equivalent diameter results provided a more reliable assessment of the ILC results. However, after this normalization step, the data scatter was still found to be large, with several statistically outlying results (Figure 1). These outliers originate from results obtained from DLS instruments equipped with different optical systems, as well from results obtained on undiluted (1 mg/mL) and diluted aliquots.

If one compares the laboratories' results (Figure 1) with the nominal or certified value ( $19.0 \text{ nm} \pm 0.6 \text{ nm}$ ) of the original material (ERM-FD100), additional outliers can be identified. This observation was somehow unexpected because, on the one hand, all these NPs have a near-monodisperse particle size distribution and sample preparation is rather straightforward, especially for laboratories using DLS on almost a routine basis. On the other hand, the 19 nm silica NPs originate from a certified reference material with a demonstrated stability and between-unit homogeneity. These features, which are usually not assessed for regular test materials, make the 19 nm silica material highly suitable for use in ILC studies. Since such degree of discrepancy has not been observed for the 50 nm PS-NH<sub>2</sub> and 50 nm PS-COOH samples (see further), it can be assumed that the biased results of the 19 nm silica particles are most likely a material issue rather than a measurement issue. Certainly, the producer of ERM-FD100, which is the base material of the 19 nm silica NPs, recommends analyzing the material as-received and immediately upon opening of the glass ampoule. The colloidal silica suspension of ERM-FD100 is originally contained in gas tight glass ampoules with their headspaces consisting of argon gas. ERM-FD100 has a very low buffer capacity and flushing the ampoules with an inert gas before closing prevents carbon dioxide from the air from dissolving, hence affecting the dispersion pH, and ultimately maintaining the colloidal stability of the suspension. During our study, the colloidal integrity of the original suspension may have unintentionally been compromised by splitting the material into different aliquots and by diluting the prepared samples to a concentration of 1 mg/mL. Moreover, since the different laboratories diluted the samples in different ways, or did not dilute them at all, some of the differences could arise from further pH changes or by contamination (for instance dilution with unfiltered water).

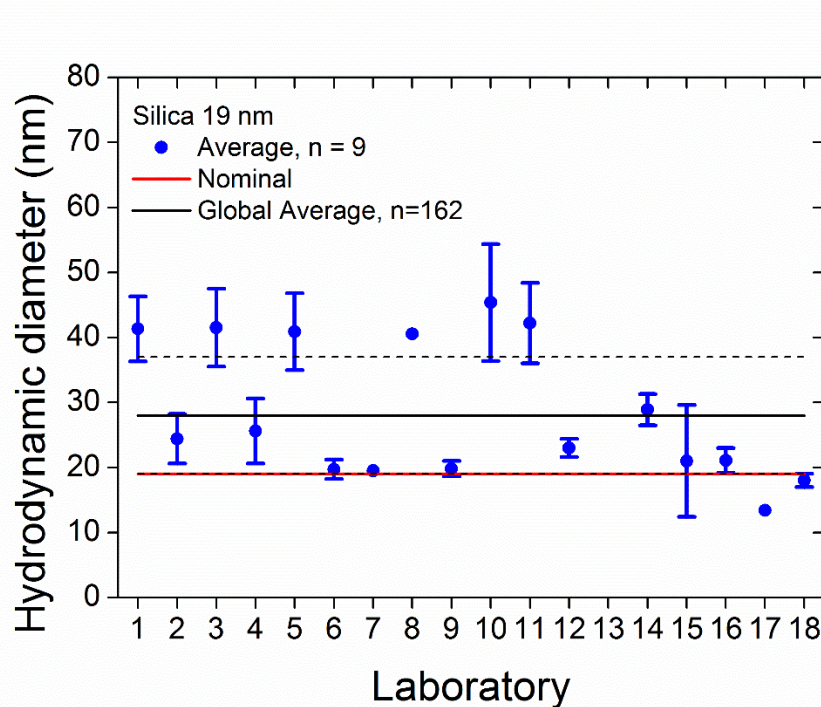


Figure 1. Results from the first ILC round by DLS. Scattered light intensity-weighted harmonic mean hydrodynamic diameter results (after correcting for particle radii) of 19 nm silica NPs dispersed in water. Dashed lines correspond to  $\pm 2 \times \text{ILC SD}$ ; error bars correspond to  $\pm 1 \times \text{lab SD}$ .

Compared to the ILC results of the 19 nm silica NPs, significantly better between-laboratory reproducibility was obtained for both the 50 nm PS-NH<sub>2</sub> and 50 nm PS-COOH NPs (figures 2a and 2b).

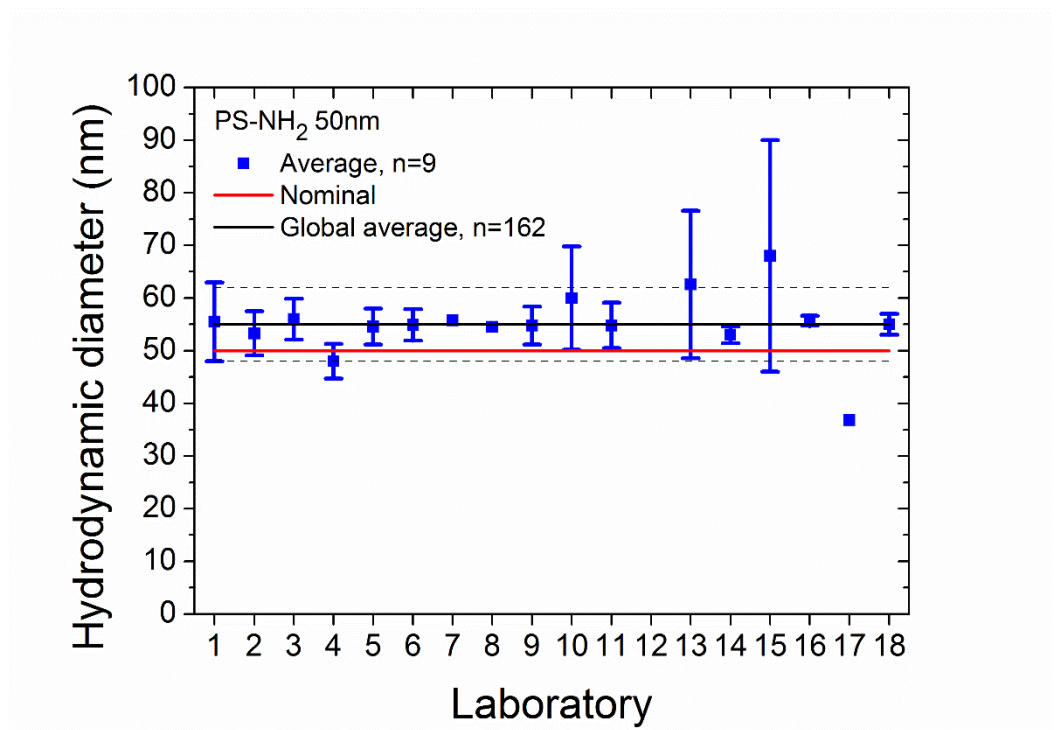


Figure 2a. Results from the first ILC round by DLS. Scattered light intensity-weighted harmonic mean hydrodynamic diameter results of 50 nm PS-NH<sub>2</sub> particles dispersed in water. Dashed lines correspond to  $\pm 2 \times$  ILC SD; error bars correspond to  $\pm 1 \times$  lab SD.

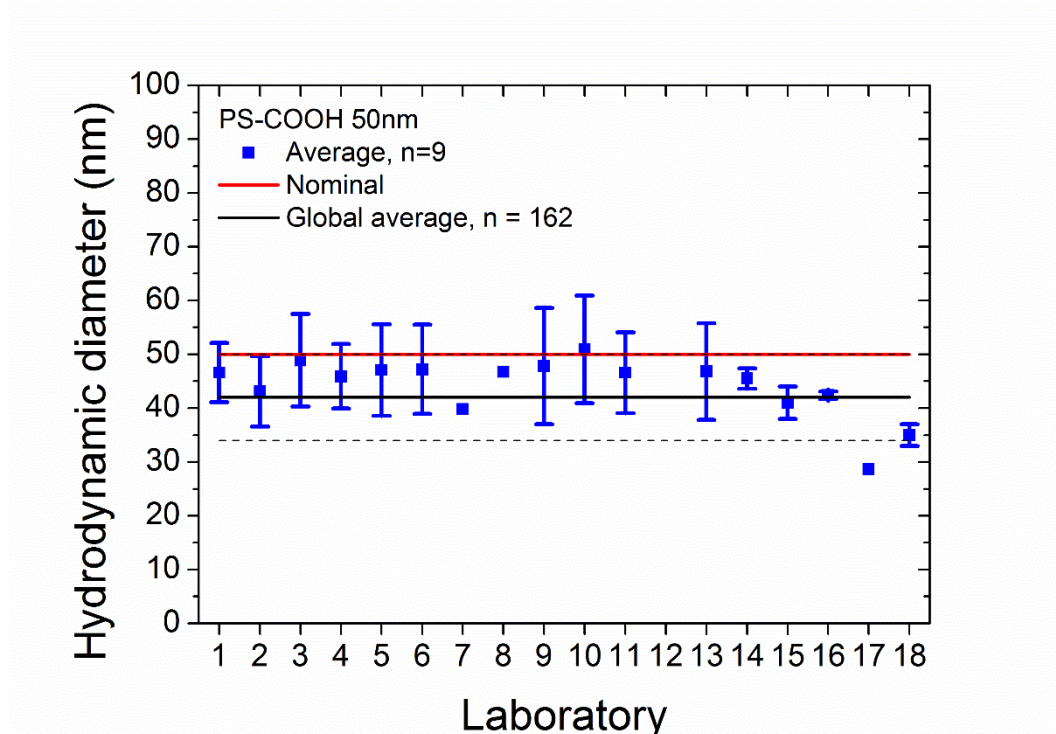


Figure 2b. Results from the first ILC round by DLS. Scattered light intensity-weighted harmonic mean hydrodynamic diameter result of the 50 nm PS-COOH particles dispersed in water. Dashed lines correspond to  $\pm 2 \times$  ILC SD; error bars correspond to  $\pm 1 \times$  lab SD.

We note that a few data points are missing because some laboratories performed only part of the measurements (Lab 13 in Figure 1, Lab 12 in Figures 2a and 2b). Additionally, the data points from the labs 7, 8 and 11 do not have error bars, because the software used by these laboratories did not compute PDI values. These laboratories quoted that for their measurements, a measurement uncertainty of less than 10% can be assumed. These uncertainties are consistent with those reported by the other laboratories. It is interesting to note the existence of these differences across available commercial instruments.

Given the observed variability, especially for the smaller NPs, it was then decided to perform a second round of ILC experiments, but this time laboratories had to conduct measurements according to a well-established SOP. The participants of the first ILC were asked to submit additional details on their measurement procedures, in order to capture differences in the procedures applied and potential sources of variability. The response rate was high (15 out of the 18 participants responded). The information obtained allowed critical points in the sample preparation and measurement procedure to be defined, which could significantly affect the reproducibility of the results. This information was then used to develop an SOP. The suitability of the developed SOP was first tested during a small round robin study in which three selected laboratories participated.

The final SOP (see supplementary information, SI) prescribed requirements regarding sample storage temperature (e.g. to avoid agglomeration), dust elimination through filtration, and sample homogenization by vortexing. These measures had to be taken before diluting the samples and starting the measurements. Indeed, the colloidal state of simple suspensions, such as those studied in the presented contribution, can alter due to changing environmental conditions. For example, temperature fluctuations or thermal gradients can cause constituent NPs to form agglomerates. These agglomerated constituent particles, normally held together by weak van der Waals forces, can relatively be easily broken by the application of moderate forces, e.g., using vortexing. It is well-known that colloidal systems can also contain aggregates. Aggregates are distinguished from agglomerates in that aggregates are held together by fusion bonds and cannot be easily fragmented. For this reason, it is known that aggregates are mainly formed during NP synthesis. For the rather simple NP systems studied during the ILCs, it can be safely assumed that aggregates have not been formed during the ILCs. Overall, it is important to stress that the vortexing conditions, prescribed by the SOPs, were particularly established for the NPs used in the study which –as previously mentioned, were selected exactly because of their simple dispersion procedure and known stability. Different NPs may require more complex dispersion procedures. Thus, the SOP provided should be amended accordingly if other NPs or media should be tested.

The NP concentration of the different test samples was chosen (1 mg/mL for 19 nm silica and 0.1 mg/mL for 50 nm PS NPs) in order to obtain a good signal-to-noise ratio in the raw data of all the DLS instruments. It must be noted that for DLS instruments with a different optical system, the aforementioned concentrations may not necessarily be optimal. Also, the signal-to-noise ratio depends on the combination of NP size, concentration and material refractive index. In particular for unknown materials, ISO 22412:2017 recommends to perform a series of measurements at concentrations over several orders of magnitude.

The developed SOP was finally distributed to the participants. The second ILC round involved only 11 laboratories (for non-technical reasons). In addition to the aforementioned 19 nm silica, 50 nm PS-NH<sub>2</sub> and PS-COOH NPs, laboratories were also asked to measure an aqueous dispersion of silica NPs with a nominal diameter of 100 nm (see Materials and methods section and SI for further details).

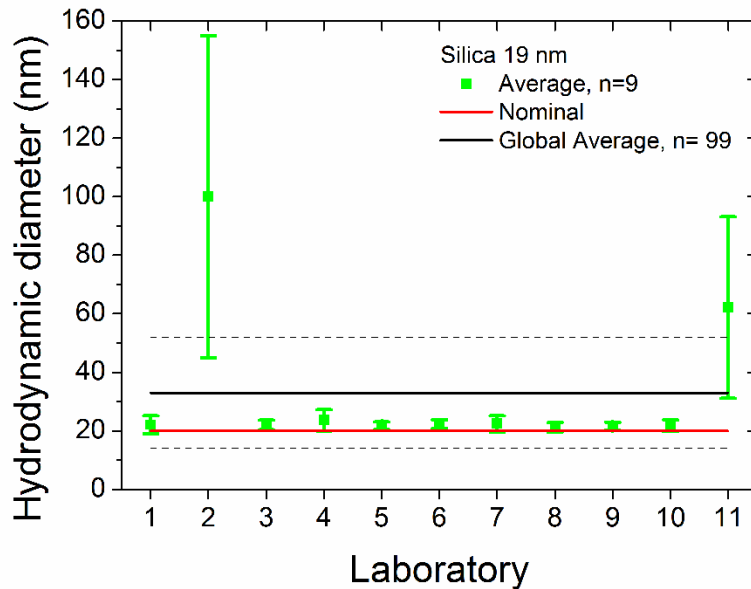


Figure 3a. Results from the second DLS round. Scattered light intensity-weighted harmonic mean hydrodynamic diameter results of 19 nm silica particles dispersed in water. Dashed lines correspond to  $\pm 2 \times$  ILC SD; error bar correspond to  $\pm 1 \times$  lab SD.

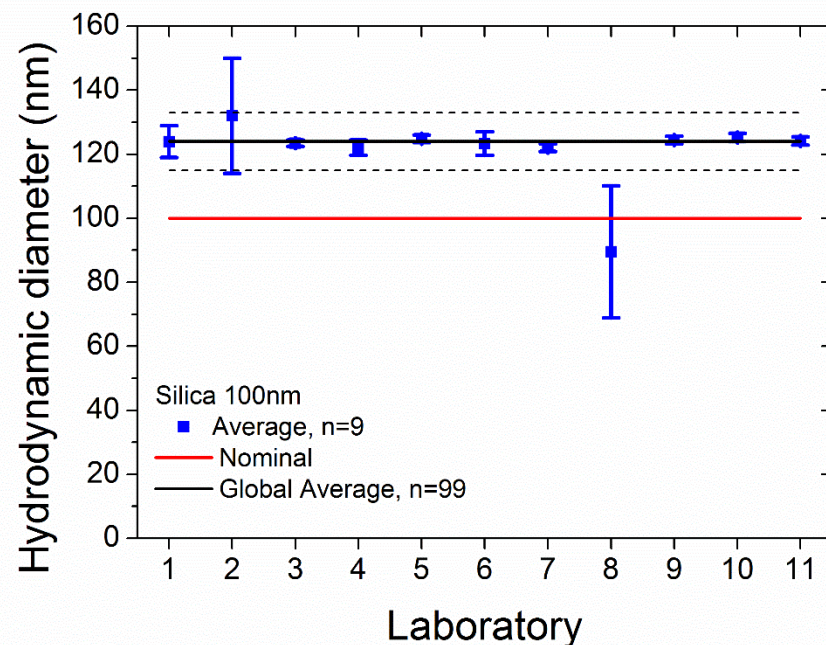


Figure 3b. Results from the second DLS round. Scattered light intensity-weighted harmonic mean hydrodynamic diameter results of 100 nm silica NPs dispersed in water. Dashed lines correspond to  $\pm 2 \times$  ILC SD; error bars correspond to  $\pm 1 \times$  lab SD.

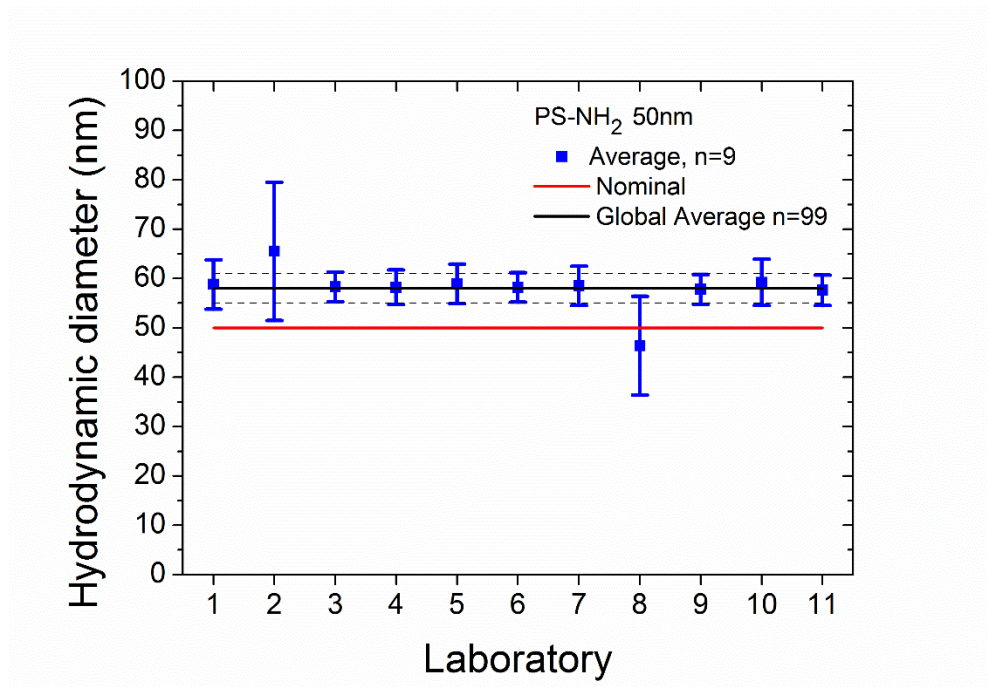


Figure 3c. Results from the second DLS round. Scattered light intensity-weighted harmonic mean hydrodynamic diameter results of 50 nm PS-NH<sub>2</sub> NPs dispersed in water. Dashed lines correspond to  $\pm 2 \times$  ILC SD; error bars correspond to  $\pm 1 \times$  lab SD.

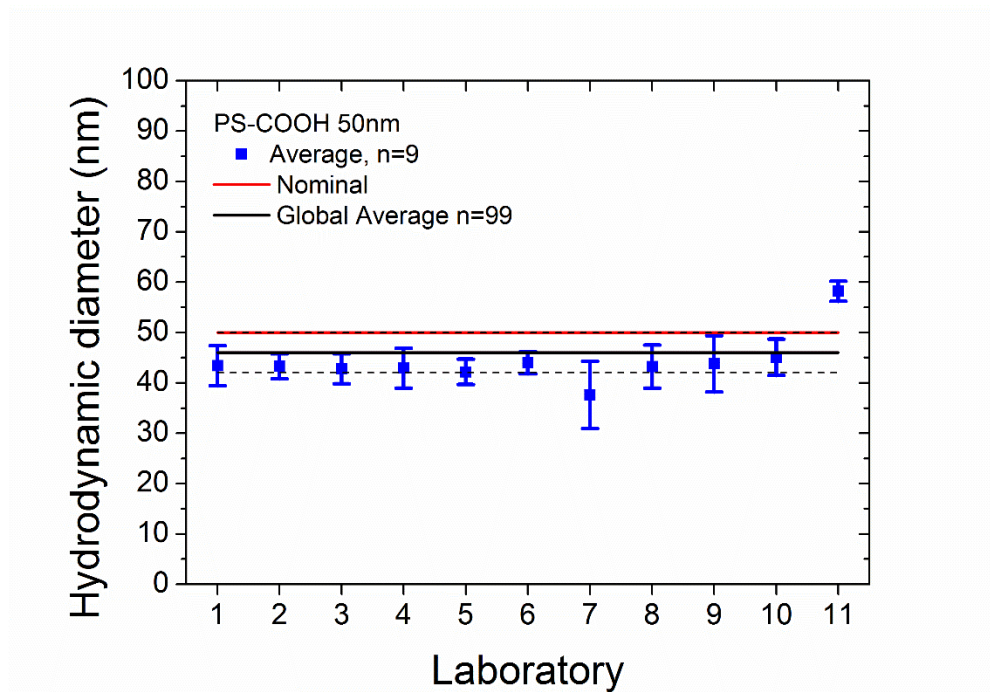


Figure 3d. Results from the second ILC round by DLS. Scattered light intensity-weighted harmonic mean hydrodynamic diameter results of 50 nm PS-COOH NPs dispersed in water. Dashed lines correspond to  $\pm 2 \times$  ILC SD; error bars correspond to  $\pm 1 \times$  lab SD.

The results of the second ILC round for the four samples are shown in Figure 3a-d (we note that because all the participating laboratories were not the same than in the first ILC, the identification numbers used in the figures are different). The new set of results clearly demonstrates the

importance and benefit of providing an optimized SOP to laboratories that participate in an ILC study, i.e. the results of almost all laboratories now either overlap, or fall within, the  $\pm 2 \times \text{SD}$  band.

For the nominal 19 nm silica NP, the results of the second ILC study (Fig. 3a) have significantly improved. Except for two results, all the other mesh around the central lines, indicating the global average of the ILC study and the nominal value of the material. Also the within-laboratory variability (i.e. error bars) has become significantly smaller for most laboratories. It is obvious that for the given material, the availability of a fit-for-purpose SOP improved both the reproducibility and repeatability of the DLS cumulants method. Despite the SOP, two results (Lab 2 and Lab 11) are outside the  $\pm 2 \times \text{SD}$  band. Both outliers also have much larger error bars, indicating that measurement and/or sample preparation problems are most likely the cause of the variability rather than a pure statistical reason. Indeed, the optical system of the DLS instrument used by Lab 2 appeared to lack sensitivity for accurate measurement of the 19 nm silica NPs at the given particle concentration, i.e. the low signal-to-noise ratio of the measurement signal erroneously affected the performance of the data analysis algorithms. Lab 11 and 8, however, used similar instruments than those used by other participants reporting comparable results. Therefore, an instrument related reason must be excluded. Since the measurement biases observed for these two laboratories were not systematic, sample preparation issues may be assumed as plausible reasons for the deviating results.

While laboratories struggled to analyze the 19 nm silica material during the first ILC round, a reasonably good reproducibility for the two 50 nm polystyrene test materials was already obtained at the time. As can be seen in Fig. 3c and 3d, the application of an SOP did hence not significantly improve the between-laboratory variability for the given materials. Regarding PS-COOH NPs, the global average increased from about 42 nm (ILC 1) to about 46 nm (ILC 2) due to one detected outlier (Lab 11). Because of the absence of technical reasons, this outlier could not be excluded from the dataset. Overall, all the results revolved around 45 nm, agreed within their stated measurement uncertainties (error bars), except for 3 outliers (lab 17, 18 of 1<sup>st</sup> ILC and – as already mentioned - lab 11 of 2<sup>nd</sup> ILC). Lab 2 used a different commercial instrument than all the others. Essentially, the instrument performed poorly for the given particle concentration: the signals were of less quality and the algorithms used introduced errors. Lab 8 and 11 used the same instrument than most other participants, and we could not elucidate why their results were different. In the case of Lab 11, the data point for PS-COOH NPs was too high, possibly due to accidental agglomeration or dust contamination. Overall, the measurement uncertainties of the results of the second ILC are remarkably more consistent and have become significantly smaller, meaning that the within-laboratory repeatability has been improved.

It is important to stress that the 50 nm PS and 100 nm silica NP samples had to be measured in water after dilution to a concentration of 0.1 mg/mL. Laboratories were instructed to analyze the 19 nm silica NP samples at the concentration of 1 mg/mL, as provided by the ILC organizer (see SOP in SI). During the small round robin study, which preceded the second ILC study, it was found that the intensity of the light scattered by the 19 nm silica sample, when diluted to 0.1 mg/mL, was below the limit of detection of some DLS instruments.

Based on the results of the two ILC rounds and the intermediate small round robin study, as well as the measurement details provided by the laboratories that participated in the first ILC round, it can be concluded that different interpretations of seemingly logical terms such as 'particle size' and

sample handling issues were major sources of uncertainty that significantly contributed to the between- and within-laboratory variability. As mentioned earlier, during the first ILC round, few laboratories considered radius as measurand while most others reported particle diameters instead. Also, except for the 19 nm silica NPs, which had to be stored at  $(18 \pm 5)^\circ\text{C}$ , no instructions were provided regarding the storage of the materials prior to the analysis. As a result, some laboratories stored the samples in a refrigerator (at  $4^\circ\text{C}$ ) while others kept the samples at room temperature. As explained before, temperature fluctuations may induce particle agglomeration. In combination with a rather mild homogenization process, de-agglomeration may have been incomplete for those samples, and as a result, the larger particles/clusters present in the sample aliquots may have affected the performance of the data algorithms. Furthermore, during the first ILC study, some laboratories diluted the dispersions by factors ranging from 10 to 1000, while others performed measurements on the as-received suspensions. The given types of particles scatter light only weakly, and if a too high dilution factor is applied then the signal-to-noise ratio can become problematic. Also, not all laboratories used water of the same quality (i.e. potential presence of particulate matter).

### ***3.1.2. DLS of NP dispersions in cell culture medium containing serum***

Given the success obtained by measuring the size of NPs dispersed in water with the use of an SOP, a new SOP was developed to characterize the dispersions as applied to biological systems, such as cells. These dispersions are typically prepared in cell culture media containing serum. Standard cell culture media are often solutions of high ionic strength, buffered at physiological pH and supplemented with, usually, 10 % fetal bovine serum (or similar amounts) as a source of nutrients for cells. This corresponds to roughly (4-6) mg/mL proteins (depending on the batch). It is known that the addition of such biological fluids can lead to the adsorption of proteins on the NP surface and the formation of a biomolecule corona which drives much of the interactions with cells<sup>5a, 6e, 22</sup>. Exposure to complex biological fluids also frequently leads to particle agglomeration. Both single particles and agglomerates can have a significantly different impact on the cellular response. It is, therefore, crucial to ensure that NP stability is also maintained when dispersed in such complex biological fluids before testing NP effects on cells.

During the first stage, the effectiveness of the developed SOP for size measurements in serum was again tested and optimized by three laboratories. After that, a new ILC exercise was organized, with participants adhering to the SOP provided (see SI). The test NPs, which had to be dispersed in the cell culture medium containing serum, were the nominal 50 nm polystyrene NPs (both with  $\text{NH}_2$  and  $\text{COOH}$  groups on their surface) and the nominal 100 nm silica NPs. The nominal 19 nm silica NPs was excluded from this ILC round because the serum proteins could interfere with the measurements due to their comparable sizes. In order to avoid variability due to the use of different serum batches, all the participating laboratories received an aliquot from a common stock of already-made cell culture medium containing serum. The SOP also included detailed instructions for storage of the samples received and – importantly – the dispersion preparation procedure. In particular, when dispersing NPs in such complex biological fluids, the crucial factor to be taken into account is not only the dispersion procedure but also the timing between dispersion and measurement. We also noted that, regarding the dispersion in water, the chosen NPs allowed very straightforward procedures for dispersion in cell culture medium containing serum: for these samples, in fact, simple vortexing

enabled formation of stable dispersions. However, this may have been different if other types of NPs had been tested. In such case, the SOP should be modified to include relevant details.

All the eight participating laboratories used commercial DLS instruments with seven of them being of the same make. The instrument used by laboratory 2 was from a different manufacturer. The results obtained during this ILC are shown in Figure 4.

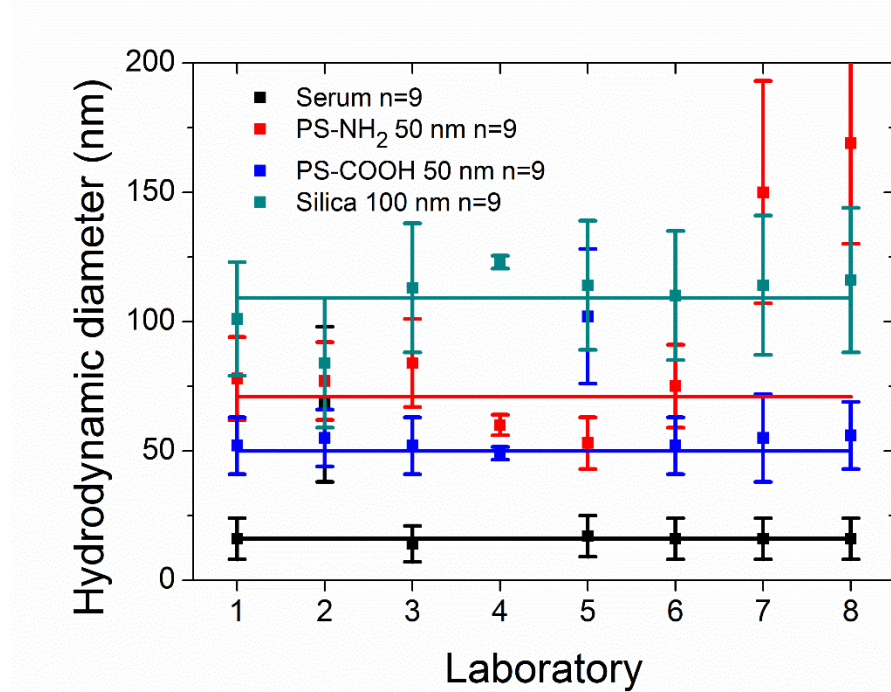


Figure 4. Results from the third ILC round by DLS. Scattered light intensity-weighted harmonic mean hydrodynamic diameter results of the NPs measured in cell culture medium containing serum. Green triangles: silica 100 nm; red circles: PS-NH<sub>2</sub> NPs; blue triangles: PS-COOH NPs, black squares: cell culture medium containing serum alone (here labeled as “serum”). Lines represent the global averages (n=63) of each sample in their respective color scheme.

A good agreement was found between the DLS results from the different laboratories, even for NPs dispersed in a complex biological medium. Regarding PS-NH<sub>2</sub>, Lab 7 and Lab 8 reported values which were significantly higher than those reported by the other laboratories. Despite the recommended precautions that had to be taken during the preparation of the test aliquots, it is not unlikely that the deviating results could be caused by the presence of agglomerates often formed due to the high ionic strength of the medium and the alteration of pH, which can have a large effect on the particles' zeta potential<sup>23</sup>. A meaningful signal could also be detected from the blank cell culture medium, due to the presence of proteins in the solution (average hydrodynamic diameter around 15 nm). Overall, the addition of serum and the ultimate adsorption of the protein molecules on the NP surface led to an increase in the average diameter due to corona formation. However, stable dispersions obtained across the different laboratories resulted in reproducible results. This is a good example of how DLS can provide valuable information, even on NP dispersions in cell culture medium as they are applied to cells.

### 3.2. DCS results

Differential centrifugal sedimentation (DCS) is a powerful technique for NP sizing. Commercial instruments for this method are available and are increasingly used in NP testing laboratories. For monodisperse NPs, DLS and DCS tend to give similar results. However, in the case of particle agglomeration or samples which are characterized by a high degree of polydispersity, DLS often detects only the agglomerates or the largest NPs, while DCS allows different sub-populations of agglomerates and the eventual presence of individual NPs to be resolved<sup>24,10a, 10e, 25</sup>.

Like the first DLS ILC round, in the first DCS ILC round no SOPs were provided to the participants regarding sample handling, the number of measurements or data reporting. Each laboratory used their in-house developed measurement and data reporting procedures, and was aware of only the type of test materials received: silica ( $\text{SiO}_2$ ), carboxylated polystyrene (PS-COOH) and amine-modified polystyrene (PS-NH<sub>2</sub>) NPs. Only three laboratories participated, with one of them unable to analyze the materials provided, even when operating the DCS instrument at its maximum rotational speed of 24000 rpm. The mass-based modal particle size results obtained by the two other laboratories during this first ILC are shown in Table 1. As can be seen, these results do not agree. It must be noted that the PS-NH<sub>2</sub> NPs appeared to be unstable during the measurements, likely due to the amine groups interacting with the sucrose molecules of the density gradient. Hence, it was decided not to pursue further the DCS measurements for the PS-NH<sub>2</sub> NPs.

NP hydrodynamic diameter (nm)	Lab 1	Lab 2
Silica (nominal 19 nm)	$26 \pm 1$	$82 \pm 6$
PS-COOH (nominal 50 nm)	$48 \pm 3$	77
PS-NH <sub>2</sub> (nominal 50 nm)	$61 \pm 6$	$19 \pm 8$

Table 1. Mass-based hydrodynamic modal diameters measured using DCS for three test NPs during the first ILC round.

Given the significant discrepancies, an SOP was again established. The dispersions received were not diluted and used at the concentration provided, 1 mg/mL. In developing and optimizing a suitable SOP for DCS testing, less challenging NPs were preferred, i.e. near-spherical particles with a not too small size and the effective density not too low. For this purpose, silica NPs of 100 nm in diameter were selected. For the given test material, a dedicated SOP was established. This SOP fixed, among others, parameters such as the rotational speed and type of sucrose density gradient. The SOP also included the critical material properties such as effective density and the complex refractive index of the silica particles, as well as a detailed description of the measurand (i.e. modal value of a logarithmically-spaced mass-based particle size distribution) and a measurement scheme (i.e. 3 consecutive measurement days with 3 replicates per day).

The second ILC round involved four laboratories with the objective of measuring the nominal 100 nm silica NPs according to the SOP. The results obtained are shown in Figure 5. Each data point corresponds to the mean of 9 replicate results of the requested measurand.

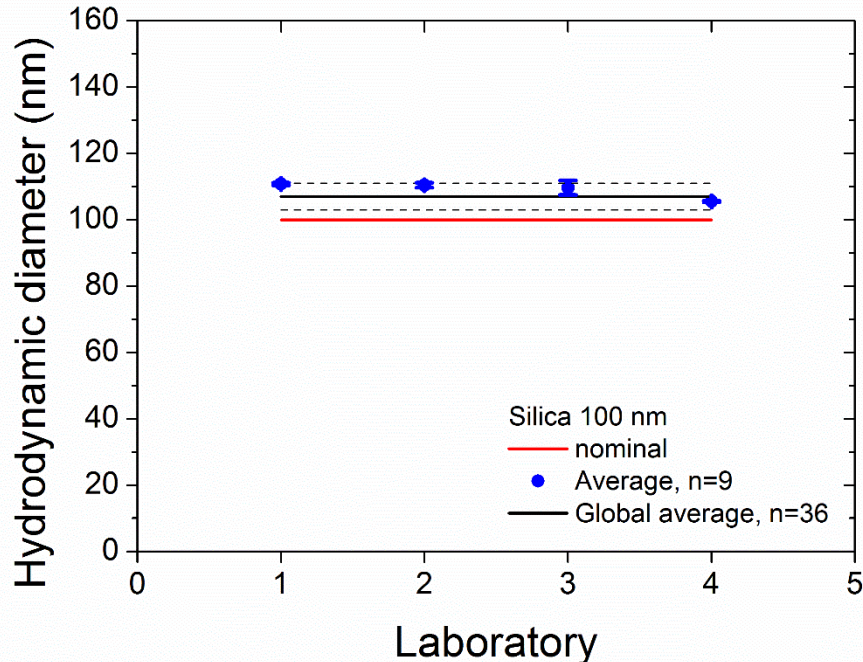


Figure 5. Results from the second ILC round by DCS. Mass-based hydrodynamic modal diameter results of 100 nm silica particles dispersed in water. Dashed lines correspond to  $\pm 2 \times$  ILC SD; error bars correspond to  $\pm 1 \times$  lab SD.

A global average of 107 nm with a standard deviation of 2 nm was obtained. This result is close to the nominal diameter of 100 nm. The results of the second ILC study are summarized in Table 2. The highly reproducible results obtained on the 100 nm silica NPs during the second ILC round demonstrated the effectiveness of the SOP. To check whether this SOP could also provide reproducible results for smaller NPs with a lower effective density (i.e. 50 nm PS-COOH), a third ILC round was organized, this time with six participating laboratories. The nominal 100 nm silica particles and the nominal 50 nm PS-COOH NPs, which were unsuccessfully analyzed during the first ILC round, had to be measured. Because of the different physical properties, a slightly adapted SOP was used for analyzing the PS-COOH NPs.

The results of the third round ILC are shown in Figures 6a and 6b. The size calculated for the silica NPs was  $(112 \pm 2)$  nm, and for the PS-COOH 50 nm NPs  $(52 \pm 5)$  nm. In the case of silica NPs, the differences between the global average and the nominal diameter could be attributed mainly to Lab 1, with the average value being an outlier and thus moving the global average to higher values. The use of the SOP for the 50 nm PS-COOH NPs resulted in a global average which almost coincided with material's nominal diameter, likely due to the consistency of its density value, particle sphericity and stability of the sample. The deviating result reported by laboratory 3 for 50 nm PS-COOH NPs is unclear. Since the laboratory obtained comparable results for 100 nm silica NPs, it can be assumed that the poor repeatability is due to a sample preparation or storage issue rather than a pure

measurement capability issue. As reflected by the small intra-laboratory standard deviations, all laboratories showed an impressive measurement precision for both samples.

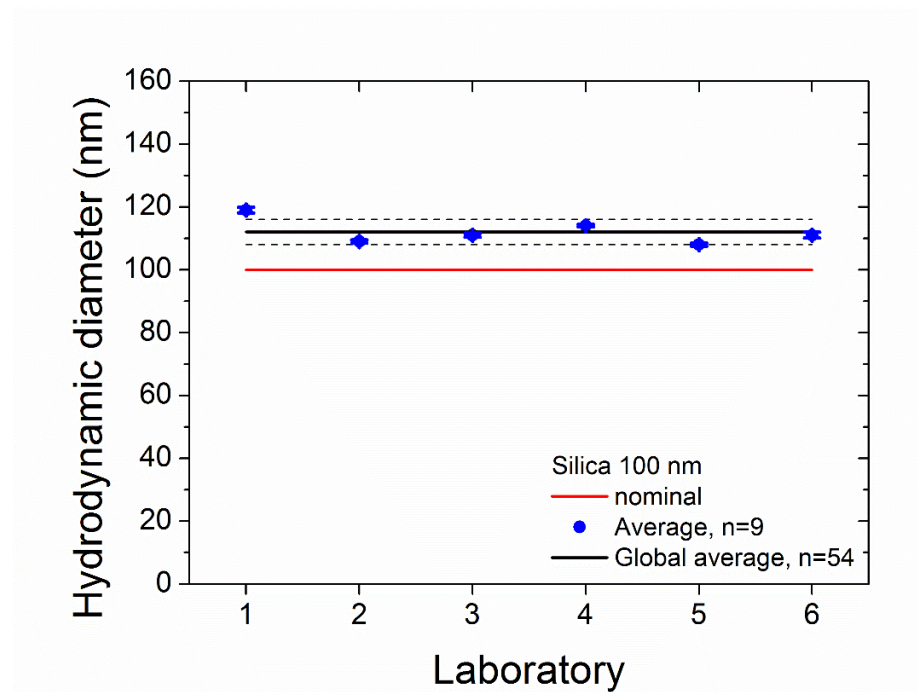


Figure 6a. Results from the third ILC round by DCS. Mass-based hydrodynamic modal diameter results of 100 nm silica NPs dispersed in water. Dashed lines correspond to  $\pm 2 \times$  ILC SD; error bars correspond to  $\pm 1 \times$  lab SD.

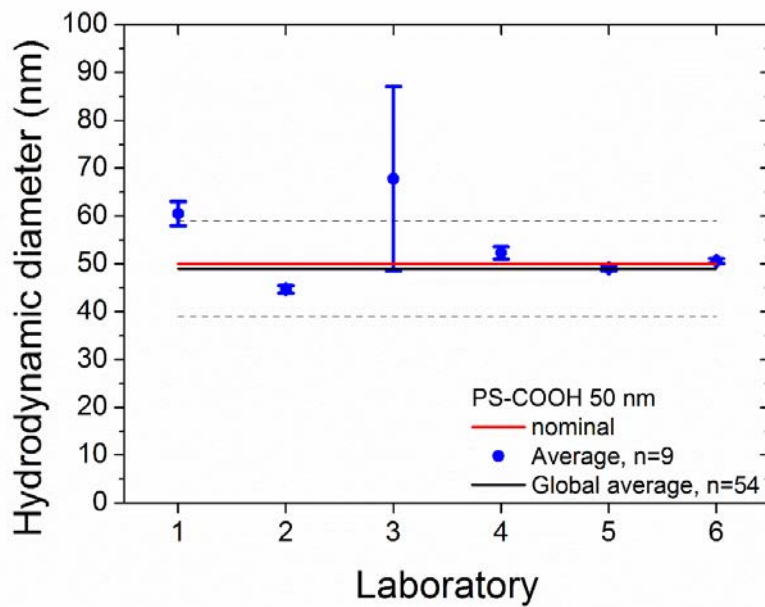


Figure 6b. Results from the third ILC round by DCS. Mass-based hydrodynamic modal diameter results for 50 nm PS-COOH NPs dispersed in water. Dashed lines correspond to  $\pm 2 \times$  ILC SD; error bars correspond to  $\pm 1 \times$  lab SD.

### 3.3. Comparison of DLS and DCS results

The results obtained for DLS and DCS with an established SOP are compiled in Table 2. In particular, the same 100 nm silica and 50 nm PS-COOH NPs were used for the second DLS and DCS rounds. This allows us to additionally compare the results obtained on the same samples with the two different methods following the established SOPs.

Technique	ILC round	Test material	Dispersant	Nominal diameter (nm)	Measured hydrodynamic diameter (nm)	CV (%)
DLS	1	SiO <sub>2</sub>	water	19	28 ± 5	17.9
DCS	1	SiO <sub>2</sub>	water	19	28 ± 39	139.3
DLS	1	PS-COOH	water	50	55 ± 3	5.5
DCS	1	PS-COOH	water	50	56 ± 16	28.6
DLS	1	PS-NH <sub>2</sub>	water	50	42 ± 4	9.5
DCS	1	PS-NH <sub>2</sub>	water	50	46 ± 22	47.8
DLS	2	SiO <sub>2</sub>	water	19	21 ± 5	23.8
DLS	2	SiO <sub>2</sub>	water	100	124 ± 4	3.2
DCS	2	SiO <sub>2</sub>	water	100	107 ± 2	1.9
DLS	2	PS-COOH	water	50	46 ± 2	4.4
DLS	2	PS-NH <sub>2</sub>	water	50	58 ± 2	3.4
DCS	3	SiO <sub>2</sub>	water	100	112 ± 2	1.8
DCS	3	PS-COOH	water	50	52 ± 5	5.8
DLS	3	SiO <sub>2</sub>	cell culture medium containing serum	100	108 ± 5	4.6
DLS	3	PS-COOH	cell culture medium containing serum	50	50 ± 15	30.0
DLS	3	PS-NH <sub>2</sub>	cell culture medium containing serum	50	69 ± 14	20.3

Table 2. Overview of DLS and DCS results obtained on different test NPs during the ILC studies. Note that for the 1<sup>st</sup> round no SOPs were used. The column *Measured hydrodynamic diameter (nm)* presents the global average ± 1 SD. CV: coefficient of variation.

As the results presented in this article reveal, the use of well-established SOPs have a positive impact on the performance of the DLS and the DCS methods for NP size analysis of near-monodisperse materials, which are dispersed in a simple matrix such as purified water. Exception of the 19 nm silica NPs, the coefficient of variation (CV), which is the quantitative expression of the between-laboratory variability or the inter-laboratory reproducibility, calculated for the different ILC rounds (Table 2), is found to be < 6%. Recently, in a similar effort also performed within the QualityNano Research Infrastructure, Hole et al. have shown that the use of SOPs can improve the reproducibility of NP size measurements using particle tracking analysis (PTA)<sup>15</sup>. For similar types of test NPs, and by using an SOP, CV values of about 10% (for 100 nm plain silica NPs in water) and 9% (for 100 nm carboxylated polystyrene NPs in water) were achieved. Our results are in line with those reported by Hole et al. and they confirm that well-established SOPs are indispensable when assessing the reproducibility of a measurement procedure.

There was no major variation across the laboratories, given separate aliquots of the same NPs, different instruments, varying shipping and storage conditions, and for independent measurements of separate dispersions within the same laboratories. These facts together suggest that each laboratory, when following the developed SOPs, could reliably measure the average size of the dispersed NPs. The small remaining differences evidenced among the laboratories could be

attributed to minute variations in the working conditions of the equipment, quality of particle size standards used to calibrate the DCS detector, sample manipulation, or sample shipment and storage. The use of the SOPs also improved the within-laboratory precision such as the method's repeatability. The latter even resulted in the detection of significant, but irrelevant, day-to-day variation for the DCS results which were reported by lab 5 and lab 4 during the third ILC rounds on the 100 nm silica and 50 nm PS-COOH particles dispersed in water.

The use of serum significantly increases the complexity of the measurement environment and adds additional uncertainty contributions which affect the overall accuracy of the final measurement results. The developed DLS SOP was shown to also be sufficiently robust for the 100 nm silica NPs when dispersed in serum. However, for the polymeric NPs in serum the CV values increased to 20% and more, demonstrating that the SOP was less performant for measuring this type of NPs in serum. The high between-laboratory variability may be attributed due to unstable interactions between the surface functional groups of the polystyrene particles with the protein molecules.

In the case of DCS, the issue of particle agglomeration would result in the appearance of subpopulations, thus even agglomeration could be measured separately from the non-agglomerated single particles. It has been previously observed, for instance, that even for samples where in DLS no strong agglomeration was identified, but higher PDI were obtained, DCS could instead show the presence of a main population of individual MPs but also few small agglomerates<sup>24</sup>. Thus it is anyway important to cautiously interpret the results obtained by DLS in serum, such as shown here and when possible the combination of different sizing methods can be extremely useful, since each method presents limitations and advantages, as discussed above.

#### 4. Conclusions

Size is essential information in NP testing, and the nanosafety community has highlighted the importance of careful characterization of NP size and stability during NP toxicity studies. Extensive efforts have been made over the past years to establish protocols and standardized procedures to ensure reproducibility in NP characterization, starting, not only with the determination of NP size in buffer and relevant media, but also their uptake, impact, and behavior on cells. Within this framework, we show here that even for relatively simple measurements of NPs in water, without standardized protocols for measurement, differences in handling procedure, instruments used, sample preparation, etc. can lead to high variability in NP size results. Thus, inter-laboratory comparisons for particle size measurements of dispersions of monodisperse spherical NPs were conducted using DLS and DCS techniques. The scopes of the ILC studies covered in this contribution are broader compared to those of previous studies. Here, up to 18 different laboratories participated in these efforts, and we could collect results obtained using seven different types of DLS instruments, four different types of monodisperse NPs, dispersed in two different dispersing media, i.e. water and a more complex model biological medium (i.e. cell culture medium containing serum).

Our results, in agreement with results from previous studies, highlight the importance of the establishment of fit-for-purpose standard operating procedures prior to measurements. The SOPs included specific instructions regarding sample storage (controlled temperature), handling and preparation (filtration of water and vortexing), all to minimize the formation of NP agglomerates.

Since particle agglomeration strongly depends on NP material, size and shape, the SOP used is specific to the particles studied (in particular the vortexing conditions). However, the developed SOPs may be used as a starting point for designing SOPs for other types of NPs. We also show that the size of NPs in biological fluids can also be measured by DLS if carefully handled and if agglomeration is avoided. This provides valuable information on dispersion stability as used for cell culture studies.

Overall, while the use of common SOPs improves the reproducibility among several laboratories, the delicate nature of handling NP dispersions remains an issue. These dispersions are metastable, and small changes in environmental conditions can induce particle agglomeration. This can particularly affect the performance of the DLS method which is highly sensitive to the presence of large particles: even a small number of large particles can significantly bias the size determination. DCS is not as strongly sensitive to agglomeration than DLS. However, also for DCS, SOPs were found necessary to harmonize key steps such as preparation of sucrose gradients and input of material and fluid physical parameters.

When using DLS or DCS, it is also important to avoid extreme dilutions, as additional uncertainties may be introduced when the measurement signals become too noisy. The concentrations used in this work were in the upper range of typical concentrations used when studying nano-bio interactions (from a maximum of 100 µg/mL down to  $\leq$ 1 µg/mL). The lower concentration range is below the limit of detection of DLS or DCS and other techniques, such as PTA, should be used instead <sup>15</sup>.

Overall this work has shown the importance of developing robust SOPs for NP size measurements and the power of ILC studies to test such SOPs across different laboratories. The SOPs have demonstrated their effectiveness for the selected test NPs that were investigated during the ILCs. However, it must be noted that, before turning such, or other, SOPs into internationally accepted standardized procedures, a full between-laboratory validation study is required. Traditional ILC studies usually focus only on the reproducibility aspect while validation studies also quantify other critical method performance characteristics such as trueness, limit of detection and quantification, robustness, linearity and sensitivity. The SOPs provided by QualityNano are available to the community to support similar efforts and as a starting material to be adapted for different NPs and dispersions of similar complexity.

## Acknowledgements

This work has been supported by the EU FP7 Capacities project QualityNano (grant no. INFRA-2010-262163). We are grateful to Sergio Anguissola, M. Zeghal, A. Dybowska, E. Isak, S. Schaaf, M. Cieślak, A. Wenk, S. Lucas, M. Nocuñ, A. Jacobs, S.K. Misra, J. Forsgren, M. Giesberg, E. Rojas, S. Patel, S. Lawson and K. Steenson for their help during the measurements. We also acknowledge the participation of the following laboratories (not in the authors' list): Natural History Museum, London; Angstrom Microstructure Laboratory Myfab, Uppsala University, Sweden; Bayer Technology Services GmbH, Leverkusen, Germany; CIC biomaGUNE, Unidad Biosuperficies, San Sebastián, Spain; Institute of Particle Science and Engineering, Faculty of Engineering, University of Leeds, England. The authors also thank E. Duh (JRC) for proofreading this manuscript.

## References

1. (a) Li, Y.; Lin, T.-y.; Luo, Y.; Liu, Q.; Xiao, W.; Guo, W.; Lac, D.; Zhang, H.; Feng, C.; Wachsmann-Hogiu, S.; Walton, J. H.; Cherry, S. R.; Rowland, D. J.; Kukis, D.; Pan, C.; Lam, K. S., A smart and versatile theranostic nanomedicine platform based on nanoporphyrin. *Nature Communications* **2014**, *5*, 4712; (b) Yohan, D.; Chithrani, B. D., Applications of Nanoparticles in Nanomedicine. *Journal of Biomedical Nanotechnology* **2014**, *10* (9), 2371-2392.
2. Salvati, A.; Pitek, A. S.; Monopoli, M. P.; Prapainop, K.; Bombelli, F. B.; Hristov, D. R.; Kelly, P. M.; Åberg, C.; Mahon, E.; Dawson, K. A., Transferrin-functionalized nanoparticles lose their targeting capabilities when a biomolecule corona adsorbs on the surface. *Nature Nanotechnology* **2013**, *8* (2), 137-143.
3. Oberdorster, G.; Cherian, M. G.; Baggs, R. B., Correlation between cadmium-induced pulmonary carcinogenicity, metallothionein expression, and inflammatory processes - a species comparison. *Environmental Health Perspectives* **1994**, *102*, 257-263.
4. Donaldson, K.; Murphy, F. A.; Duffin, R.; Poland, C. A., Asbestos, carbon nanotubes and the pleural mesothelium: a review of the hypothesis regarding the role of long fibre retention in the parietal pleura, inflammation and mesothelioma. *Particle and Fibre Toxicology* **2010**, *7*.
5. (a) Nel, A. E.; Maedler, L.; Velegol, D.; Xia, T.; Hoek, E. M. V.; Somasundaran, P.; Klaessig, F.; Castranova, V.; Thompson, M., Understanding biophysicochemical interactions at the nano-bio interface. *Nature Materials* **2009**, *8* (7), 543-557; (b) Zhang, H.; Dunphy, D. R.; Jiang, X.; Meng, H.; Sun, B.; Tarn, D.; Xue, M.; Wang, X.; Lin, S.; Ji, Z.; Li, R.; Garcia, F. L.; Yang, J.; Kirk, M. L.; Xia, T.; Zink, J. I.; Nel, A.; Brinker, C. J., Processing Pathway Dependence of Amorphous Silica Nanoparticle Toxicity: Colloidal vs Pyrolytic. *Journal of the American Chemical Society* **2012**, *134* (38), 15790-15804; (c) Wang, F.; Bexiga, M. G.; Anguissola, S.; Boya, P.; Simpson, J. C.; Salvati, A.; Dawson, K. A., Time resolved study of cell death mechanisms induced by amine-modified polystyrene nanoparticles. *Nanoscale* **2013**, *5* (22), 10868-10876; (d) Anguissola, S.; Garry, D.; Salvati, A.; O'Brien, P. J.; Dawson, K. A., High Content Analysis Provides Mechanistic Insights on the Pathways of Toxicity Induced by Amine-Modified Polystyrene Nanoparticles. *Plos One* **2014**, *9* (9), e108025; (e) Guarneri, D.; Sabella, S.; Muscetti, O.; Belli, V.; Malvindi, M. A.; Fusco, S.; De Luca, E.; Pompa, P. P.; Netti, P. A., Transport across the cell-membrane dictates nanoparticle fate and toxicity: a new paradigm in nanotoxicology. *Nanoscale* **2014**, *6* (17), 10264-10273; (f) Sabella, S.; Carney, R. P.; Brunetti, V.; Malvindi, M. A.; Al-Juffali, N.; Vecchio, G.; Janes, S. M.; Bakr, O. M.; Cingolani, R.; Stellacci, F.; Pompa, P. P., A general mechanism for intracellular toxicity of metal-containing nanoparticles. *Nanoscale* **2014**, *6* (12), 7052-7061; (g) De Matteis, V.; Malvindi, M. A.; Galeone, A.; Brunetti, V.; De Luca, E.; Kote, S.; Kshirsagar, P.; Sabella, S.; Bardi, G.; Pompa, P. P., Negligible particle-specific toxicity mechanism of silver nanoparticles: The role of Ag<sup>+</sup> ion release in the cytosol. *Nanomedicine-Nanotechnology Biology and Medicine* **2015**, *11* (3), 731-739.
6. (a) Zhu, Y.; Li, W.; Li, Q.; Li, Y.; Li, Y.; Zhang, X.; Huang, Q., Effects of serum proteins on intracellular uptake and cytotoxicity of carbon nanoparticles. *Carbon* **2009**, *47* (5), 1351-1358; (b) Ge, C.; Du, J.; Zhao, L.; Wang, L.; Liu, Y.; Li, D.; Yang, Y.; Zhou, R.; Zhao, Y.; Chai, Z.; Chen, C., Binding of blood proteins to carbon nanotubes reduces cytotoxicity. *Proceedings of the National Academy of Sciences* **2011**, *108* (41), 16968-16973; (c) Hu, W.; Peng, C.; Lv, M.; Li, X.; Zhang, Y.; Chen, N.; Fan, C.; Huang, Q., Protein Corona-Mediated Mitigation of Cytotoxicity of Graphene Oxide. *ACS Nano* **2011**, *5* (5), 3693-3700; (d) Lesniak, A.; Fenaroli, F.; Monopoli, M. P.; Åberg, C.; Dawson, K. A.; Salvati, A., Effects of the Presence or Absence of a Protein Corona on Silica Nanoparticle Uptake and Impact on Cells. *ACS Nano* **2012**, *6* (7), 5845-5857; (e) Monopoli, M. P.; Åberg, C.; Salvati, A.; Dawson, K. A., Biomolecular coronas provide the biological identity of nanosized materials. *Nature Nanotechnology* **2012**, *7* (12), 779-786.
7. (a) Guarneri, D.; Malvindi, M. A.; Belli, V.; Pompa, P. P.; Netti, P., Effect of silica nanoparticles with variable size and surface functionalization on human endothelial cell viability and angiogenic

activity. *Journal of Nanoparticle Research* **2014**, *16* (2), 2229; (b) Orts-Gil, G.; Natte, K.; Drescher, D.; Bresch, H.; Mantion, A.; Kneipp, J.; Oesterle, W., Characterisation of silica nanoparticles prior to in vitro studies: from primary particles to agglomerates. *Journal of Nanoparticle Research* **2011**, *13* (4), 1593-1604.

8. (a) Cho, E. C.; Zhang, Q.; Xia, Y. N., The effect of sedimentation and diffusion on cellular uptake of gold nanoparticles. *Nature Nanotechnology* **2011**, *6* (6), 385-391; (b) Feliu, N.; Sun, X.; Alvarez Puebla, R. A.; Parak, W. J., Quantitative Particle-Cell Interaction: Some Basic Physicochemical Pitfalls. *Langmuir* **2017**, *33* (27), 6639-6646.
9. Kestens, V.; Roebben, G.; Herrmann, J.; Jamting, A.; Coleman, V.; Minelli, C.; Clifford, C.; De Temmerman, P. J.; Mast, J.; Liu, J. J.; Babick, F.; Colfen, H.; Emons, H., Challenges in the size analysis of a silica nanoparticle mixture as candidate certified reference material. *Journal of Nanoparticle Research* **2016**, *18* (6), 171.
- 10.(a) Monopoli, M. P.; Walczyk, D.; Campbell, A.; Elia, G.; Lynch, I.; Bombelli, F. B.; Dawson, K. A., Physical-Chemical Aspects of Protein Corona: Relevance to in Vitro and in Vivo Biological Impacts of Nanoparticles. *Journal of the American Chemical Society* **2011**, *133* (8), 2525-2534; (b) Bell, N. C.; Minelli, C.; Tompkins, J.; Stevens, M. M.; Shard, A. G., Emerging Techniques for Submicrometer Particle Sizing Applied to Stober Silica. *Langmuir* **2012**, *28* (29), 10860-10872; (c) Cascio, C.; Gilliland, D.; Rossi, F.; Calzolai, L.; Contado, C., Critical Experimental Evaluation of Key Methods to Detect, Size and Quantify Nanoparticulate Silver. *Analytical Chemistry* **2014**, *86* (24), 12143-12151; (d) Kelly, P. M.; Aberg, C.; Polo, E.; O'Connell, A.; Cookman, J.; Fallon, J.; Krpetic, Z.; Dawson, K. A., Mapping protein binding sites on the biomolecular corona of nanoparticles. *Nature Nanotechnology* **2015**, *10* (5), 472-479; (e) Lozano, O.; Mejia, J.; Masereel, B.; Toussaint, O.; Lison, D.; Lucas, S., Development of a PIXE analysis method for the determination of the biopersistence of SiC and TiC nanoparticles in rat lungs. *Nanotoxicology* **2012**, *6* (3), 263-271.
- 11.(a) Shapero, K.; Fenaroli, F.; Lynch, I.; Cottell, D. C.; Salvati, A.; Dawson, K. A., Time and space resolved uptake study of silica nanoparticles by human cells. *Molecular BioSystems* **2011**, *7* (2), 371-378; (b) Kim, J. A.; Salvati, A.; Aberg, C.; Dawson, K. A., Suppression of nanoparticle cytotoxicity approaching in vivo serum concentrations: limitations of in vitro testing for nanosafety. *Nanoscale* **2014**, *6* (23), 14180-14184.
12. Anderson, W.; Kozak, D.; Coleman, V. A.; Jamting, A. K.; Trau, M., A comparative study of submicron particle sizing platforms: Accuracy, precision and resolution analysis of polydisperse particle size distributions. *Journal of Colloid and Interface Science* **2013**, *405*, 322-330.
- 13.(a) Lamberty, A.; Franks, K.; Braun, A.; Kestens, V.; Roebben, G.; Linsinger, T. P. J., Interlaboratory comparison for the measurement of particle size and zeta potential of silica nanoparticles in an aqueous suspension DISCUSSION. *Journal of Nanoparticle Research* **2011**, *13* (12), 7317-7329; (b) Roebben, G.; Ramirez-Garcia, S.; Hackley, V. A.; Roesslein, M.; Klaessig, F.; Kestens, V.; Lynch, I.; Garner, C. M.; Rawle, A.; Elder, A.; Colvin, V. L.; Kreyling, W.; Krug, H. F.; Lewicka, Z. A.; McNeil, S.; Nel, A.; Patri, A.; Wick, P.; Wiesner, M.; Xia, T.; Oberdorster, G.; Dawson, K. A., Interlaboratory comparison of size and surface charge measurements on nanoparticles prior to biological impact assessment. *Journal of Nanoparticle Research* **2011**, *13* (7), 2675-2687.
14. Braun, A.; Kestens, V.; Franks, K.; Roebben, G.; Lamberty, A.; Linsinger, T. P. J., A new certified reference material for size analysis of nanoparticles. *Journal of Nanoparticle Research* **2012**, *14* (9), 1021.
15. Hole, P.; Sillence, K.; Hannell, C.; Maguire, C. M.; Roesslein, M.; Suarez, G.; Capracotta, S.; Magdolenova, Z.; Horev-Azaria, L.; Dybowska, A.; Cooke, L.; Haase, A.; Contal, S.; Mano, S.; Vennemann, A.; Sauvain, J. J.; Staunton, K. C.; Anguissola, S.; Luch, A.; Dusinska, M.; Korenstein, R.; Gutleb, A. C.; Wiemann, M.; Prina-Mello, A.; Riediker, M.; Wick, P., Interlaboratory comparison of size measurements on nanoparticles using nanoparticle tracking analysis (NTA). *Journal of Nanoparticle Research* **2013**, *15* (12).
16. Wang, F.; Yu, L.; Monopoli, M. P.; Sandin, P.; Mahon, E.; Salvati, A.; Dawson, K. A., The biomolecular corona is retained during nanoparticle uptake and protects the cells from the

damage induced by cationic nanoparticles until degraded in the lysosomes. *Nanomedicine: Nanotechnology, Biology and Medicine* **2017**, *9* (8), 1159-1168.

17. Berne, B. J.; Pecora, R., *Dynamic light scattering: with applications to chemistry, biology, and physics*. Dover Publications: 2000.

18. Phillips, G. D. J., Contribution of non-hydrodynamic interactions to the concentration-dependence of the friction factor of the mutual diffusion-coefficient. *Journal of Chemical Physics* **1981**, *74* (4), 2436-2440.

19. DeLoid, G.; Cohen, J. M.; Darrah, T.; Derk, R.; Rojanasakul, L.; Pyrgiotakis, G.; Wohllaben, W.; Demokritou, P., Estimating the effective density of engineered nanomaterials for in vitro dosimetry. *Nature Communications* **2014**, *5*.

20. Kestens, V.; Coleman, V. A.; De Temmerman, P.-J.; Minelli, C.; Woehlecke, H.; Roebben, G., Improved Metrological Traceability of Particle Size Values Measured with Line-Start Incremental Centrifugal Liquid Sedimentation. *Langmuir* **2017**, *33* (33), 8213-8224.

21. Langevin, D.; Raspaud, E.; Mariot, S.; Knyazev, A.; Stocco, A.; Salonen, A.; Luch, A.; Haase, A.; Trouiller, B.; Relier, C.; Lozano, O.; Thomas, S.; Salvati, A.; Dawson, K., On the measurement of nanoparticle size using Dynamic Light Scattering. Advantages and drawbacks of commercial instruments. *submitted for publication to NanolImpact*.

22. (a) Cedervall, T.; Lynch, I.; Lindman, S.; Berggard, T.; Thulin, E.; Nilsson, H.; Dawson, K. A.; Linse, S., Understanding the nanoparticle-protein corona using methods to quantify exchange rates and affinities of proteins for nanoparticles. *Proceedings of the National Academy of Sciences of the United States of America* **2007**, *104* (7), 2050-2055; (b) Roecker, C.; Poetzl, M.; Zhang, F.; Parak, W. J.; Nienhaus, G. U., A quantitative fluorescence study of protein monolayer formation on colloidal nanoparticles. *Nature Nanotechnology* **2009**, *4* (9), 577-580; (c) Maiorano, G.; Sabella, S.; Sorce, B.; Brunetti, V.; Malvindi, M. A.; Cingolani, R.; Pompa, P. P., Effects of Cell Culture Media on the Dynamic Formation of Protein-Nanoparticle Complexes and Influence on the Cellular Response. *Ac Nano* **2010**, *4* (12), 7481-7491; (d) Walkey, C. D.; Chan, W. C. W., Understanding and controlling the interaction of nanomaterials with proteins in a physiological environment. *Chemical Society Reviews* **2012**, *41* (7), 2780-2799; (e) Tenzer, S.; Docter, D.; Kuharev, J.; Musyanovych, A.; Fetz, V.; Hecht, R.; Schlenk, F.; Fischer, D.; Kiouptsi, K.; Reinhardt, C.; Landfester, K.; Schild, H.; Maskos, M.; Knauer, S. K.; Stauber, R. H., Rapid formation of plasma protein corona critically affects nanoparticle pathophysiology. *Nature Nanotechnology* **2013**, *8* (10), 772-U1000.

23. Sikora, A.; Bartczak, D.; Geissler, D.; Kestens, V.; Roebben, G.; Ramaye, Y.; Varga, Z.; Palmai, M.; Shard, A. G.; Goenaga-Infante, H.; Minelli, C., A systematic comparison of different techniques to determine the zeta potential of silica nanoparticles in biological medium. *Analytical Methods* **2015**, *7* (23), 9835-9843.

24. Walczyk, D.; Bombelli, F. B.; Monopoli, M. P.; Lynch, I.; Dawson, K. A., What the Cell "Sees" in Bionanoscience. *Journal of the American Chemical Society* **2010**, *132* (16), 5761-5768.

25. Contado, C.; Mejia, J.; Garcia, O. L.; Piret, J. P.; Dumortier, E.; Toussaint, O.; Lucas, S., Physicochemical and toxicological evaluation of silica nanoparticles suitable for food and consumer products collected by following the EC recommendation. *Analytical and Bioanalytical Chemistry* **2016**, *408* (1), 271-286.